Hydrogenation and Ring Opening of Tetralin on Supported Nickel Zirconium-Doped Mesoporous Silica Catalysts. Influence of the Nickel Precursor

ARTICLE *in* LANGMUIR · MAY 2003

Impact Factor: 4.46 · DOI: 10.1021/la020865l

5 AUTHORS, INCLUDING:

Dolores Eliche-Quesada
Universidad de Jaén
36 PUBLICATIONS **396** CITATIONS
SEE PROFILE

Pedro Maireles-Torres
University of Malaga
120 PUBLICATIONS **2,223** CITATIONS
SEE PROFILE

Enrique Rodriguez-Castellon
University of Malaga
399 PUBLICATIONS **5,340** CITATIONS
SEE PROFILE

Hydrogenation and Ring Opening of Tetralin on Supported Nickel Zirconium-Doped Mesoporous Silica Catalysts. Influence of the Nickel Precursor

D. Eliche-Quesada, J. Mérida-Robles, P. Maireles-Torres, E. Rodríguez-Castellón, and A. Jiménez-López*

Departamento de Química Inorgánica, Cristalografía y Mineralogía, Facultad de Ciencias, Universidad de Málaga, Campus de Teatinos, 29071 Málaga, Spain

Received October 21, 2002. In Final Form: February 18, 2003

When mesoporous silica doped with zirconium with a MCM-41-type structure as a support was used, three different supported nickel catalysts were prepared by means of incipient wetness impregnation using different nickel salt solutions. Impregnation with aqueous or ethanolic nickel nitrate solutions gives rise to large Ni particles, whereas with an aqueous nickel citrate solution, the formation of small particles with a high metallic area is observed. Therefore, the use of nickel citrate as the nickel source effectively inhibits the aggregation of nickel particles. This catalyst showed the highest catalytic activity in the hydrogenation and ring opening of tetralin at a moderate temperature (648 K) and high hydrogen pressure (6 MPa), exhibiting a THN conversion of 90% with a high yield of hydrogenation products (53.8%) and cracking compounds (36.1%).

Introduction

The aromatics in diesel fuel not only produce undesired emissions in the exhaust gases but also decrease the cetane number. This has led to new tighter regulations concerning the fuel quality and exhaust emissions and, consequently, the conversion of the hydrogenation of aromatics in an essential step in the oil refining process, directed toward the production of environmentally friendly fuels. The fuel quality can be met by deep hydrotreating, which typically consists of a two-stage process, with a conventional hydrotreating catalyst at the first stage and a more active hydrogenation catalyst in the second one.[1]

Currently, the catalysts used for decreasing the percentages of aromatics are based on NiW and NiMo[2−11] and noble metals[12−17] supported on alumina, zeolites, etc. These studies have shown the importance of the nature of the support in regards to the catalytic performance. In past years, the use of MCM-41 solids as catalytic supports has resulted in significant improvements for many reactions when compared to conventional and commercial catalysts. That is why many research groups are using mesoporous MCM-41-type silica as a support instead of alumina, amorphous silica−alumina, or zeolites.[13,18−23] The family of mesoporous MCM-41 materials presents attractive properties, such as uniform pore size distributions and very high specific surface areas, for use as a support.[31,32]

Concerning the preparation of supported nickel catalysts for hydrogenation reactions,[11,24−29] many different supports have been used, among them Y-zeolites, α-Al_2O_3, γ-Al_2O_3, and alumina-pillared α-zirconium phosphate, but

* Author to whom correspondence should be addressed. Phone: (+34) 952131876. Fax: (+34) 952132000. E-mail: ajimenezl@uma.es.

(1) Cooper, B. H.; Donnis, B. B. L. *Appl. Catal., A* **1996**, *137*, 203.
(2) Yasuda, H.; Higo, M.; Yoshitomi, S.; Sato, T.; Imamura, M.; Matsubayashi, H.; Shimada, H.; Nishijima, A.; Yoshimura, Y. *Catal. Today* **1997**, *39*, 77.
(3) Song, C. J.; Kwak, C.; Moon, S. H. *Catal. Today* **2002**, *2676*, 1.
(4) Sato, K.; Iwata, Y.; Miki, Y.; Shimada, H. *J. Catal.* **1999**, *186*, 45.
(5) Sato, K.; Iwata, Y.; Yoneda, T.; Miki, Y.; Shimada, H. *Catal. Today* **1998**, *45*, 367.
(6) Sanford, E. C.; Steer, J. G.; Muehlenbachs, K.; Gray, M. R. *Energy Fuels* **1995**, *9*, 928.
(7) Bouchy, M.; Peureuxdenys, S.; Dyfresnes, P.; Kasztelan, S. *Ind. Eng. Chem. Res.* **1993**, *32*, 1592.
(8) Ho, T. C. *Energy Fuels* **1994**, *8*, 1149.
(9) Lure, M. A.; Kurets, I. Z.; Kushnarev, D. F.; Malyechenko, A. A.; Schimidt, F. K. *Kinet. Catal.* **2000**, *41*, 57.
(10) Ozkan, A. R.; Yanik, J.; Saglam, M.; Yeskel, M. *Energy Fuels* **1999**, *13*, 433.
(11) Hernández-Huesca, R.; Mérida-Robles, J.; Maireles-Torres, P.; Rodríguez-Castellón, E.; Jiménez-López, A. *J. Catal.* **2001**, *203*, 122.
(12) Rousset, J. L.; Stievano, L.; Cadete Santos Aires, F. J.; Geantet, C.; Renouprez, A. J.; Pellarin, M. *J. Catal.* **2001**, *202*, 163.
(13) Corma, A.; Martínez, A.; Martínez-Soria, V. *J. Catal.* **1997**, *169*, 480.
(14) Navarro, R. M.; Pawelec, B.; Trejo, J. M.; Mariscal, R.; Fierro, J. L. *J. Catal.* **2000**, *189*, 184.
(15) Hu, L.; Xia, G.; Qu, L.; Li, C.; Xin, Q.; Li, D. *J. Mol. Catal. A: Chem.* **2001**, *171*, 169.
(16) Fujikawa, T.; Idei, K.; Ebihara, T.; Mizuguchi, H.; Usui, K. *Appl. Catal. A* **2000**, *192*, 253.
(17) Corma, A.; Martínez, A.; Martínez-Soria, V. *J. Catal.* **2001**, *200*, 259.
(18) Corma, A.; Martínez, A.; Martínez-Soria, V. *J. Catal.* **1995**, *153*, 25.
(19) Reddy, K. M.; Song, C. *Catal. Today* **1996**, *31*, 137.
(20) Song, C.; Reddy, K. M. *Appl. Catal. A* **1999**, *176*, 1.
(21) Wang, A.; Wang, Y.; Kabe, T.; Chen, Y.; Ishihara, A.; Qian, W. *J. Catal.* **2001**, *199*, 19.
(22) Ramírez, J.; Contreras, R.; Castillo, P.; Klimova, T.; Zárate, R.; Luna, R. *Appl. Catal. A* **2000**, *197*, 69.
(23) Klimova, T.; Rodríguez, E.; Martínez, M.; Ramírez, J. *Microporous Mesoporous Mater.* **2001**, *44−45*, 357.
(24) Corma, A.; Iglesias, M.; Sanchez, F. *Catal. Lett.* **1995**, *32*, 313.
(25) Isoda, T.; Kusakabe, K.; Morooka, S.; Mochida, I. *Energy Fuels* **1998**, *12*, 493.
(26) Chaudhuri, S. N.; Nath, S. K.; Majumdar, D. S. *Stud. Surf. Sci. Catal.* **1998**, *113*, 793.
(27) Zhang, Z. G.; Okada, K.; Yamamoto, M.; Yoshida, T. *Catal. Today* **1998**, *45*, 361.
(28) Rautanen, P. A.; Aittamaa, J. R.; Krause, A. O. I. *Chem. Eng. Sci.* **2001**, *56*, 1247.
(29) Mérida-Robles, J.; Olivera-Pastor, P.; Rodríguez-Castellón, E.; Jiménez-López, A. *J. Catal.* **1997**, *169*, 317.
(30) Rodríguez-Castellón, E.; Díaz, L.; Braos-García, P.; Mérida-Robles, J.; Maireles-Torres, P.; Jiménez-López, A.; Vaccari, A. *Appl. Catal. A* **2003**, *240*, 83.
(31) Beck, J.; Vartuli, J. C.; Roth, W. J.; Leonowicz, M. E.; Kresge, C. T.; Schmitt, K. D.; Chu, C. T. W.; Olson, D. H.; Sheppard, E. W.; McCullen, S. B.; Higgins, J. B.; Schlenker, J. L. *J. Am. Chem. Soc.* **1992**, *114*, 10834.
(32) Kresge, C. T.; Leonowicz, M. E.; Roth, W. J.; Vartuli, J. C.; Beck, J. S. *Nature* **1992**, *359*, 710.

10.1021/la020865l CCC: $25.00
Published on Web 05/07/2003

sometimes they exhibit low hydrogenating activities due to strong nickel-supported interactions. In this sense, we have recently reported that zirconium-doped mesoporous silica is an appropriate support for metallic nickel because the metal−support interaction is moderate. However, high nickel loadings give rise to large metal particles, mainly located on the external surface of the support.[30] It has also been demonstrated that the enhanced acidity of this support favors the cracking of aromatic molecules, thus increasing the cetane number of the feedstock. Moreover, the preparation and characterization of nickel supported on mesoporous materials have been reported in several papers.[18,33−42]

On the other hand, the most extensively used method to prepare these catalysts is the impregnation with different salt solutions, such as nickel nitrate[18,33−37,41] and nickel citrate.[43−45] Thus, Lensveld et al.[45] have concluded that the incipient wetness impregnation with an aqueous nickel citrate solution is an excellent method to prepare MCM-41-supported nickel catalysts, with 10 wt % Ni and highly dispersed nickel oxide nanoparticles confined inside the pores.

The purpose of the present study is to evaluate the effect of using different impregnation nickel salt solutions on the catalytic properties of nickel supported on zirconium-doped mesoporous silica catalysts in the hydrogenation of tetralin at high hydrogen pressures. The fact than one can control the NiO particle size depending on the nickel salt solution used for the impregnation of the support is interesting. Moreover, the influence of the reaction temperature, contact time, and H_2/tetralin molar ratio will be optimized to increase the production of cracking compounds (CCs), which are responsible for the increase in the cetane number of a diesel feedstock.

Experimental Section

Materials. Zirconium-doped mesoporous silica with a Si/Zr molar ratio of 5, MCM-SiZr5, was synthesized as described elsewhere,[46] but the reaction time was reduced to only 24 h at room temperature. Powdered MCM-SiZr5 was impregnated by using the incipient wetness method. Three different nickel precursor salt solutions were tested: aqueous nickel nitrate solution, nickel nitrate ethanolic solution, and aqueous nickel citrate solution. The latter solution was prepared by mixing nickel carbonate and citric acid in a 3:2 molar ratio in deionized water and heating until the suspension turned to a bright-green solution. In all cases, the amount of nickel precursor necessary to attain a loading of about 20 wt % Ni was dissolved in the corresponding incipient volume of the chosen solvent and then incorporated onto the support in a single step. After impregnation, the solids were first dried (333 K, 12 h) and then calcined at 823 K for 4 h (1.5 K min^{-1} heating rate). Hereafter, the catalysts will be designated as Ni(Nit/A), Ni(Nit/E), and Ni(Cit/A).

Instrumental Techniques. The nickel content of the catalysts was determined by atomic absorption spectroscopy by using a Perkin-Elmer 3100 apparatus.

The powder X-ray diffraction (PXRD) patterns were obtained with a Siemens D5000 diffractometer, equipped with a graphite monochromator using Cu Kα radiation.

X-ray photoelectron spectra (XPS) were recorded on a Physical Electronics PHI 5700 spectrometer with nonmonochromatic Mg Kα radiation (300 W, 15 kV, 1253.6 eV) and a multichannel detector. The spectra of powder samples were recorded in the constant-pass energy mode at 29.35 eV, using a 720-μm-diameter analysis area. Charge referencing was measured against adventitious carbon (C 1s, 284.8 eV). A PHI Access ESCA-V6.0 F software package was used to record and analyze the spectra. A Shirley-type background was subtracted from the signals. The recorded spectra were always fitted using Gauss−Lorentz curves to determine the binding energy of the different element core levels more accurately. The reduced samples, before the XPS analysis, were kept in *n*-hexane to avoid contact with air.

Temperature-programmed reduction (H_2-TPR) experiments were carried out between 313 and 973 K, using a flow of Ar/H_2 (40 cm^3 min^{-1}, 10 vol % of H_2) and a heating rate of 10 K min^{-1}. The effluent gas was passed through a cold trap (193 K) before the thermal conductivity detector to remove water from the exit stream.

The acidic properties were analyzed by the temperature-programmed desorption of chemisorbed ammonia (NH_3-TPD). Before the adsorption of ammonia at 373 K, the samples were reduced at 723 K using a flow of H_2 (60 cm^3 min^{-1}). The ammonia desorbed between 373 and 823 K (heating rate of 10 K min^{-1}) was analyzed by an online gas chromatograph (Shimadzu GC-14A), provided with a thermal conductivity detector.

The specific surface areas of the solids were evaluated from the nitrogen adsorption−desorption isotherms at 77 K in a Quantachrom Autosorb-1 apparatus, after degassing at 473 K and 1.3 × 10^{-2} Pa for 24 h.

Hydrogen chemisorption was performed in a Micromeritics ASAP 2010 apparatus, after the in situ reduction of the samples at 723 K (15 K min^{-1}) for 1 h, under a flow of H_2. After reduction, the catalysts were degassed at 10^{-4} Pa for 10 h at the same temperature and cooled at 308 K to carry out the chemisorption of H_2. The range of pressures studied in the chemisorption was 0.013−0.04 MPa, and the amounts of hydrogen chemisorbed were calculated by extrapolation of the isotherms to zero pressure. The degree of reduction of nickel (α) was determined by oxygen chemisorption in the same apparatus. The samples were reduced and degassed under the same conditions, the oxygen chemisorption was carried out at 673 K, and the range of pressures studied was 0.013−0.08 MPa.

Transmission electron microscopy (TEM) was performed with a Phillips CM-200 high-resolution transmission electron microscope. Previously, the reduced samples were embedded in an *n*-hexane solution and suspended on a Cu grid of 3.5 mm in diameter.

Catalytic Activity Measurements. Tetralin hydrogenation was chosen as a model reaction for the hydrogenation of aromatics in diesel fuels. The reaction was performed in a high-pressure fixed-bed continuous-flow stainless-steel catalytic reactor (9.1-mm i.d. and 230-mm length) operated in the down-flow mode. The reaction temperature was measured with an interior-placed thermocouple in direct contact with the top part of the catalyst bed. The organic feed consisted of a solution of tetralin in *n*-heptane (5−20 vol %) and was supplied by means of a Gilson 307SC piston pump (model 10SC). A fixed volume of catalyst (3 cm^3 with a particle size of 0.85−1.00 mm) without dilution was used in all cases. Prior to the activity test, the catalysts were reduced in situ at atmospheric pressure with H_2 (flow rate 60 cm^3 min^{-1}) at 723 K for 1 h, with a heating rate of 15 K min^{-1}. Catalytic activities were measured at different temperatures, under 6.0 MPa of hydrogen pressure, and liquid hourly space

(33) Halachev, T.; Nava, R.; Dimitrov, L. *Appl. Catal. A* **1998**, *169*, 111.
(34) Cui, J.; Yue, Y. H.; Sun, Y.; Dong, W. Y.; Gao, Z. *Stud. Surf. Sci. Catal.* **1997**, *105*, 687.
(35) Yue, Y.; Sun, Y.; Gao, Z. *Catal. Lett.* **1997**, *47*, 167.
(36) Hartmann, M.; Pöppl, A.; Kevan, L. *J. Phys. Chem.* **1995**, *99*, 17494.
(37) Hartmann, M.; Pöppl, A.; Kevan, L. *J. Phys. Chem.* **1996**, *100*, 9906.
(38) Hartmann, M.; Pöppl, A.; Kevan, L. *Stud. Surf. Sci. Catal.* **1996**, *101*, 801.
(39) Yue, Y.; Sun, Y.; Zu, Q.; Gao, Z. *Appl. Catal. A* **1998**, *175*, 131.
(40) Ziolek, M.; Novak, I.; Kecyk, P.; Kujawa, J. *Stud. Surf. Sci. Catal.* **1998**, *177*, 509.
(41) Klimova, T.; Ramírez, J.; Calderón, M.; Domínguez, J. M. *Stud. Surf. Sci. Catal.* **1998**, *117*, 493.
(42) Junges, U.; Disser, S.; Schmid, G.; Schüth, F. *Stud. Surf. Sci. Catal.* **1998**, *117*, 391.
(43) Meima, G. R.; Dekker, B. G.; van Dillen, A. J.; Geus, J. W.; Bongaarts, J. E.; van Bure, F. R.; Delcour, K.; Wigman, J. M. *Stud. Surf. Sci. Catal.* **1987**, *31*, 83.
(44) van den Brink, P. J.; Scholten, A.; Van Wageningen, A.; Lamers, M. D. A.; van Dillen, A. J.; Geus, J. W. *Stud. Surf. Sci. Catal.* **1991**, *63*, 527.
(45) Lensveld, D. J.; Mesu, J. G.; Jos van Dillen, A.; de Jong, K. P. *Microporous Mesoporous Mater.* **2001**, *44−45*, 401.
(46) Jiménez-López, A.; Rodríguez-Castellón, E.; Maireles-Torres, P.; Díaz, L.; Mérida-Robles, J. *Appl. Catal. A* **2001**, *218*, 295.

velocities ranging between 6.0 and 12.0 h^{-1}. The H_2/tetralin molar ratio was varied between 5 and 20.0. The catalytic reaction was studied by collecting liquid samples after they remained for 45 min at each reaction temperature and were kept in sealed vials for posterior analysis by both gas chromatography (Shimadzu GC-14B, equipped with a flame ionization detector and a capillary column, TBR-1, coupled to an automatic injector Shimadzu AOC-20i) and mass spectrometry (Hewlett-Packard 5988A). The influence of the reaction parameters such as the reaction temperature, contact time, and H_2/tetralin molar ratio on the conversion and selectivity was also studied. The performance of the microreactor and accuracy of the analytical method were studied by feeding a solution of tetralin in *n*-heptane (10 vol %) to the reactor filled with 3 cm^3 of SiC, operating at 573 K and 6.0 MPa. No formation of foreign products was detected with a recovery percentage of the tetralin feed of 95%. In previous experiments, variations in the amount of catalyst and total flow rate while maintaining a constant space velocity led to no modification of the conversion values. Also, no influence of the particle diameter was found.

Results and Discussion

Characterization of the Catalysts. The characterization of the MCM-SiZr5, used as the support of the nickel catalysts, has been described elsewhere.[47,48] The PXRD patterns, at low angles, of the supported nickel catalysts before and after reduction of the nickel species, indicate that the hexagonal structure of the support is maintained after the nickel incorporation. The diffractograms of the unreduced catalysts display the characteristic diffraction lines of cubic NiO crystals at 2.41, 2.09, and 1.47 Å (Figure 1a), whereas those of the reduced catalysts show the presence of metallic nickel (2.03 and 1.76 Å; Figure 1b). In both cases, before and after reduction, the samples prepared by using nickel nitrate as the precursor salt (aqueous or ethanolic solution) exhibit sharp and well-resolved peaks, revealing that relatively large nickel oxide and metallic nickel particles are formed. However, the weak and broad reflections observed when nickel citrate is used as the impregnation salt indicate the existence of small nickel oxide and metallic nickel particles in this catalyst. This fact was previously detected by Lensveld et al.[45] by studying the influence of the nickel precursor on the characteristics of nickel supported on mesoporous silica, with a loading of 10 wt %.

The crystallite sizes (Table 1), estimated from the full width at half-maximum according to Scherrer's equation, drastically change as a function of the salt solution used in the impregnation process. Thus, by using an aqueous nickel citrate solution, the average particle sizes of NiO and Ni (9.4 and 8.4 nm, respectively) are smaller than those obtained when an aqueous (>50.0 and 21.6 nm) or ethanolic solution (42.0 and 24.2 nm) of nickel nitrate are used. It is noteworthy that the small value, 8.4 nm, corresponding to the Ni particles in the Ni(Cit/A) catalyst in comparison to the other catalysts, is only slightly lower than that obtained for the unreduced catalyst. This fact reveals that the strong interaction between the nickel oxide and support, in the case of the Ni(Cit/A) catalyst, avoids the sintering of the metal particles during the reduction process. It is well-known that the chelated nickel species, formed when nickel citrate is used as the nickel source, give rise to a wetted and highly viscous film on the surface of the support, which upon calcination is broken up and decomposed, resulting in the formation of very small nickel oxide particles.

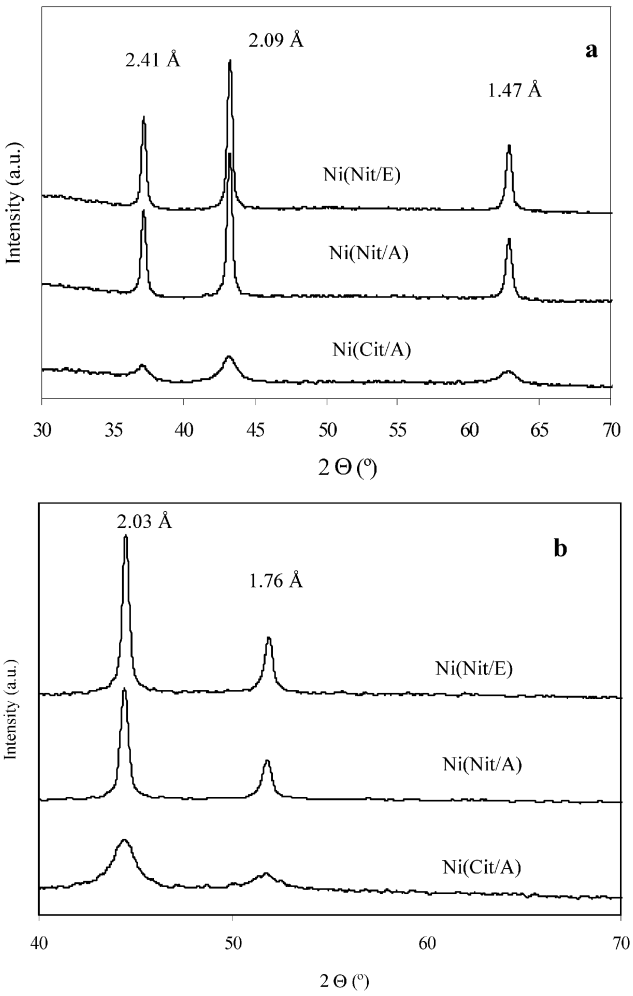

Figure 1. PXRD patterns of the (a) unreduced and (b) reduced supported nickel materials.

Table 1. Structural, Textural, and Acidic Properties of the Supported Nickel Catalysts

sample	Ni (wt %)	S_{BET} ($m^2 g^{-1}$; U)[b]	V_p ($cm^3 g^{-1}$; U)[b]	*d* (nm)[a] NiO (U)[b]	*d* (nm)[a] Ni (R)[c]	total acidity (μmol NH_3 g^{-1}; R)[c]
MCM-SiZr5		503	0.52			544
Ni(Nit/E)	22.5	244	0.21	42.0	24.2	885
Ni(Nit/A)	22.4	214	0.18	>50	21.6	930
Ni(Cit/A)	21.5	221	0.18	9.4	8.4	800

[a] Calculated from PXRD data according to Scherrer's equation. [b] U, unreduced. [c] R, reduced.

The textural characteristics of the support and unreduced catalysts were evaluated from the nitrogen adsorption−desorption isotherms (Table 1). All unreduced catalysts exhibit nitrogen isotherms with the same shape as that of the support, but a drastic reduction of the specific surface area and pore volume was observed. This decrease could be attributed not only to the presence of large NiO particles partially blocking the porous network but also to the increase in the density of the materials after the incorporation of a nickel loading as high as about 20 wt %.

On the other hand, H_2-TPR analysis is a useful technique to get information about the reducibility of the nickel oxide deposited on the MCM-SiZr5 support. The H_2-TPR profiles of the unreduced materials are different depending on the salt used in the impregnation process (Figure 2). Thus,

(47) Jones, D. J.; Jiménez-Jiménez, J.; Jiménez-López, A.; Maireles-Torres, P.; Olivera-Pastor, P.; Rodríguez-Castellón, E.; Rozière, J. *Chem. Commun.* **1997**, 431.
(48) Bianchi, O. C.; Campanati, M.; Maireles-Torres, P.; Rodríguez-Castellón, E.; Jiménez-López, A.; Vaccari, A. *Appl. Catal. A* **2001**, *220*, 105.

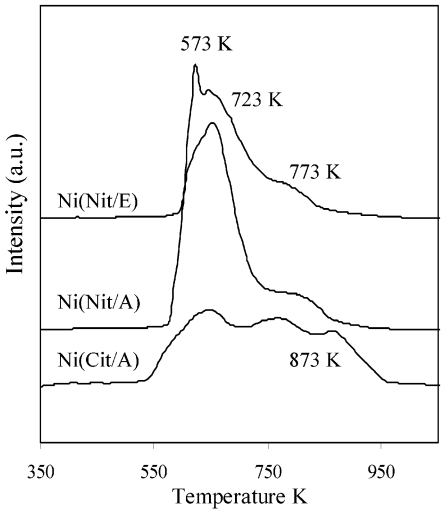

Figure 2. H_2-TPR profiles of the unreduced catalysts.

the unreduced Ni(Nit/E) and Ni(Nit/A) materials show a broad band of H_2 consumption where two maxima close to 573 and 723 K can be distinguished, together with a small shoulder at about 773 K. However, the material prepared by using Ni(Cit/A) presents a very broad signal of H_2 consumption with different maxima between 523 and 898 K. The band observed at lower temperatures, in all cases, coincides approximately with that observed in the reduction of the bulk NiO (613 K), indicating the presence of a fraction of a nickel species analogous to nickel oxide. In consequence, these NiO particles must be larger than those associated with the reduction bands appearing at higher temperatures. Accordingly, the unreduced Ni(Nit/A) and Ni(Nit/E) catalysts contain NiO particles larger than those present in the unreduced Ni(Cit/A) catalyst. However, the reduction band detected at low temperatures in this latter material also reveals the presence of a small fraction of large NiO particles, which might be mainly located on the external surface of the support, similar to the unreduced Ni(Nit/A) and Ni(Nit/E) materials, which could be responsible of the decrease observed in its surface area. The H_2-TPR curve for Ni(Cit/A) also shows H_2-consumption bands at very high temperatures, especially that observed at 873 K, indicating the existence of a strong interaction of Ni^{2+} species with the support. These H_2-TPR results are in agreement with those reported by Lensveld et al.,[45] but they used a lower nickel loading (10 wt %). Therefore, both studies are demonstrating that nickel oxide can be well dispersed on mesoporous materials by using incipient wetness impregnation with an aqueous solution of nickel citrate.

In addition, XPS has been used to study the nature of the surface species. Figure 3a shows the Ni 2p region containing the Ni $2p_{1/2}$ and Ni $2p_{3/2}$ emission lines of the unreduced Ni(Cit/A) material. The other unreduced samples showed very similar XPS spectra. The position of the Ni $2p_{3/2}$ line is characteristic of Ni^{2+} and, in all cases, can be deconvoluted into two components (Table 2). The first component (855.1−855.6 eV) can be assigned to octahedral Ni^{2+} and appears shifted to higher binding energy values with respect to the bulk NiO.[49] The second one at 857.0−857.7 eV can be associated with either some Ni^{2+} ions interacting with $M-O^-$ groups or very small crystallites of NiO located on the walls of the mesopores. The peak located at 862.6 eV, which essentially remains in the same position, corresponds to the shake-up satellite

(49) Klein, J. C.; Hercules, D. M. *J. Catal.* **1983**, *82*, 424.

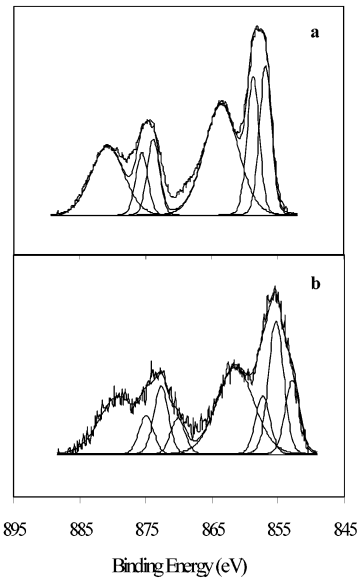

Figure 3. Ni 2p XPS spectra of the (a) unreduced and (b) reduced Ni(Cit/A) materials.

Table 2. XPS Data for the Supported Nickel Materials, before and after Reduction

	binding energy (eV)				
				Ni $2p_{3/2}$	
sample	Zr $2p_{3/2}$	Si 2p	O 1s	Ni^{2+}	Ni^0 (% Ni^0/Ni_{total})
MCM-SiZr5	182.8	102.8	532.8		
Unreduced Catalysts					
Ni(Nit/E)	182.9	103.4	532.9	855.6 857.7	
Ni(Nit/A)	182.7	103.2	532.6	855.1 857.0	
Ni(Cit/A)	182.5	102.9	532.8	855.3 857.5	
Reduced Catalysts					
Ni(Nit/E)	182.9	103.3	532.4	854.8 856.4	852.7 (25.1)
Ni(Nit/A)	182.8	103.0	532.4	855.5 857.2	853.2 (26.9)
Ni(Cit/A)	182.7	103.0	532.5	855.4 857.1	853.2 (17.3)

structure of Ni^{2+}. The binding energies of the Zr $3d_{5/2}$ and Si 2p signals are, in all cases, practically constant. In Figure 3b, the Ni 2p core-level spectrum of the reduced Ni(Cit/A) catalyst is also shown. It can be observed that the reduction of the nickel species is not completely accomplished because in addition to a new Ni $2p_{3/2}$ signal at 853.2−852.7 eV revealing the existence of metallic nickel, two other contributions at 854.8−855.5 eV and 856.4−857.2 eV reveal the existence of NiO with different degrees of interaction with the support. The percentages of nickel reduction, calculated by taking into account the integrated peak area of Ni^0 against the Ni^{II} signals (including the satellite peak), are also collected in Table 2. As is expected by considering the H_2-TPR results, the Ni(Cit/A) catalyst presents the lowest percentage of reduction (17.3%). However, the reduction degrees determined by XPS are in all cases very low, possibly as a result of the fact that the photoelectrons that emerged from the core level of nickel are subsequently reabsorbed by other nickel atoms of the metallic particles. Moreover, because it was not possible to transport the reduced samples from the reduction reactor to the spectrometer without exposure to air, the low percentage of reduced nickel observed by XPS can also be attributed to a partial

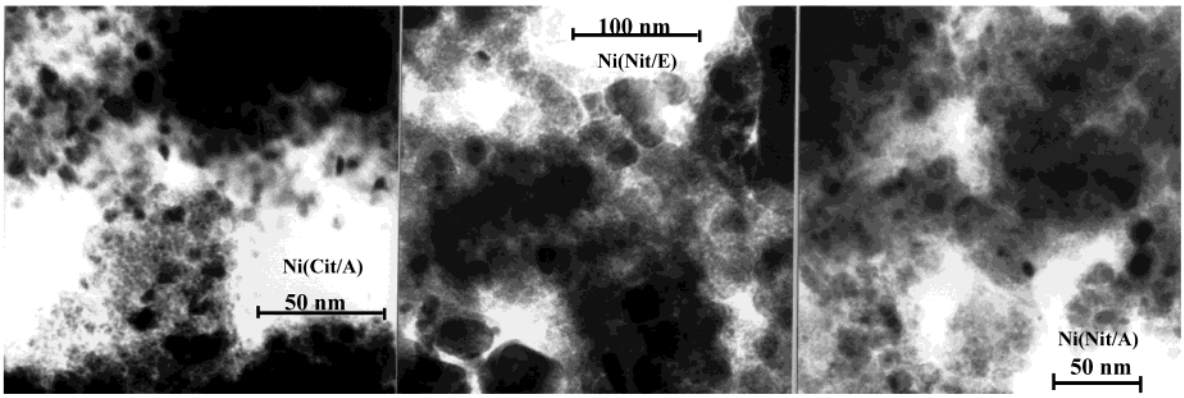

Figure 4. TEM pictures for the catalysts reduced at 723 K.

Table 3. Metallic Characteristics of the Supported Nickel Catalysts

			metallic surface		d^c (nm)	
catalyst	α^a (%)	D^b (%)	($m^2\ g_{cat}^{-1}$)	($m^2\ g_{Ni^0}^{-1}$)	H_2	TEM
Ni(Nit/E)	83.3	1.8	2.6	13.1	41.5	16.1
Ni(Nit/A)	94.4	2.5	3.7	18.7	29.1	11.3
Ni(Cit/A)	31.2	10.9	15.4	71.5	7.6	7.0

[a] α is the reduction degree determined by chemisorption of O_2. [b] D is the metallic dispersion. [c] d is the average diameter of the metallic crystallite.

oxidation of the catalysts due to this short air exposure. On the other hand, the surface atomic Ni/(Si + Zr) ratio of the unreduced materials was calculated from the integrated peak intensities of XPS to probe the distribution of the supported phases as a function of the impregnation salt used. The highest ratio, 0.40, is found for the unreduced Ni(Cit/A), which indicates the better dispersion of the NiO phase for this material, whereas the values corresponding to the other unreduced catalysts are 0.16 and 0.11 for Ni(Nit/E) and Ni(Nit/A), respectively. This evolution confirms the highest dispersion of nickel oxide on the mesoporous support when nickel citrate is employed.

The acidic properties of the reduced catalysts, determined by NH_3-TPD, are compiled in Table 1. The incorporation of nickel on the support provokes an increase in the total acidity in comparison with that of the MCM-SiZr5 support as a result of the high tendency of the remaining unreduced nickel(II) to coordinate ammonia molecules forming aminocomplexes. Curiously, the lowest total acidity is found for the Ni(Cit/A) sample, which could be justified by taking into account the better dispersion of the NiO phase on the surface of the support, thus masking a considerable number of strong acid centers.

Table 3 shows the metallic properties of the catalysts after reduction at 723 K. The degree of reduction, α, obtained by O_2 chemisorption, reflects again that complete reduction was not achieved for any catalyst, the Ni(Cit/A) catalyst being that which presents the lowest degree of reduction. This is consonant with the H_2-TPR data because the Ni(Cit/A) material was the most difficult to reduce. Under the experimental conditions used, no chemisorption of neither H_2 nor O_2 was detected on the support. As could be expected from the PXRD and H_2-TPR data, the highest percentage of metal exposed (10.9%) was obtained by impregnation with nickel citrate. On the other hand, nickel nitrate leads to slightly better dispersion if an aqueous solution is used. Anyway, the dispersion degree and the metallic surface area are always lower than those obtained for the Ni(Cit/A) catalyst.

Scheme 1

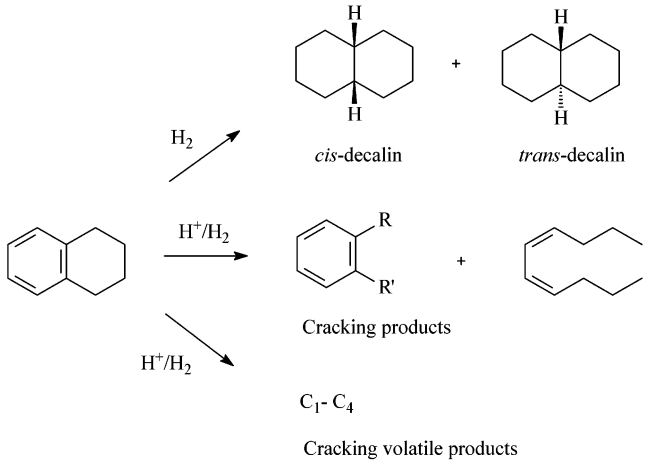

Figure 4 displays the TEM micrographs of the three catalysts. All of them exhibit a heterogeneous distribution of metal Ni particles. This technique provides average nickel particle diameter values slightly different from those obtained by PXRD and H_2 chemisorption (Table 3), but in the same way, the Ni(Cit/A) catalyst is the sample with the lowest particle size, as was previously observed by Lensveld et al.[50]

Hydrogenation of Tetralin. Tetralin hydrogenation was chosen as a model reaction to evaluate the catalytic performance of this family of supported nickel catalysts in the hydrogenation of aromatic hydrocarbons in diesel fuels. A large number of products were detected by gas chromatography analysis. After the identification of the majority of them, they were classified, as was recently reported,[30,51] into the following groups: (i) volatile compounds (VCs) that include noncondensable C_1-C_4 products that were calculated from the carbon balance of the reaction; (ii) hydrogenation products that include *trans*- and *cis*-decalins; (iii) cracking compounds that include benzene, alkylbenzenes, and polyalkylolefins; and (iv) naphthalene (Scheme 1). Products heavier than decalins were not found. This must be from taking into account that high yields of hydrogenation products, and especially CCs, produce an increase in the cetane number of fuels.

Figure 5 shows the tetralin conversion of the three catalysts at different reaction temperatures (548−648 K). The catalysts prepared by using nickel nitrate as the impregnation salt present a very similar evolution of the

(50) Lensveld, D. J.; Mesu, J. G.; van Dillen, A. J.; de Jong, K. P. *Stud. Surf. Sci. Catal.* **2002**, *143*, 647.
(51) Hernández-Huesca, R.; Mérida-Robles, J.; Maireles-Torres, P.; Rodríguez-Castellón, E.; Jiménez-López, A. *J. Catal.* **2002**, *203*, 122.

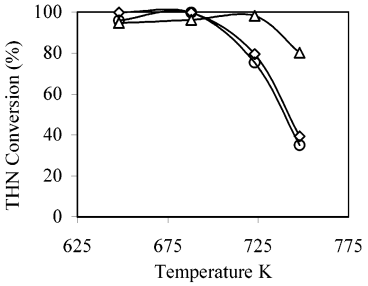

Figure 5. Conversion for tetralin hydrogenation on the (◇) Ni(Nit/E), (○) Ni(Nit/A), and (△) Ni(Cit/A) catalysts as a function of the reaction temperature. Experimental conditions: H_2/THN molar ratio = 10.1; $P(H_2)$ = 6 MPa; contact time = 3.6 s.

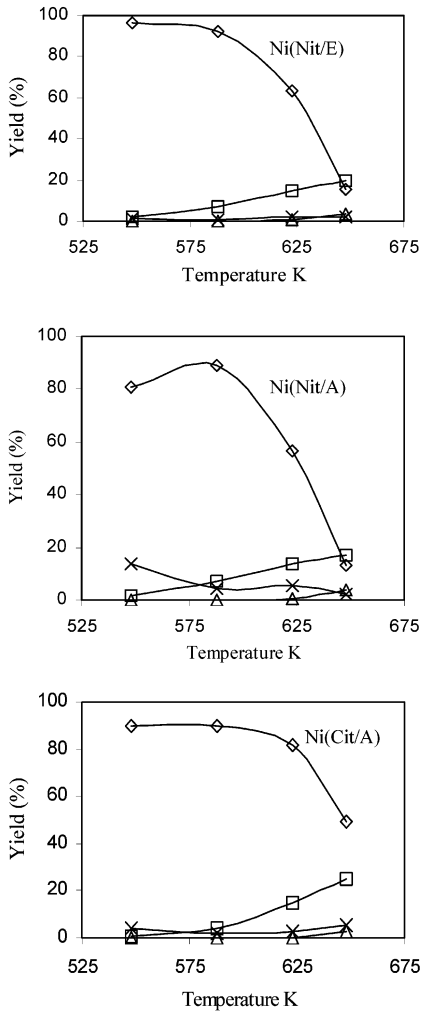

Figure 6. Evolution of the yield toward the different reaction products as a function of the reaction temperature on the three catalysts: (◇) *trans*- + *cis*-decalins, (□) CC, (△) naphthalene, and (×) VC. Experimental conditions: H_2/THN molar ratio = 10.1; $P(H_2)$ = 6 MPa; contact time = 3.6 s.

conversion with the reaction temperature, as is expected due to the analogous metallic properties of both catalysts. The conversion values are very high for both catalysts at low temperatures (548−588 K) but at 648 K drastically fall until 40% is reached. The Ni(Cit/A) catalyst exhibits roughly the same behavior at low temperatures, but this catalyst still maintains a very high conversion (98.1−80.1%) at high reaction temperatures (623−648 K). The decrease of the conversion with the temperature is due to thermodynamic reasons because the hydrogenation of tetralin is an exothermic reaction and, therefore, is favored at low temperatures.[13,16,52,53] For this reason, the yield of

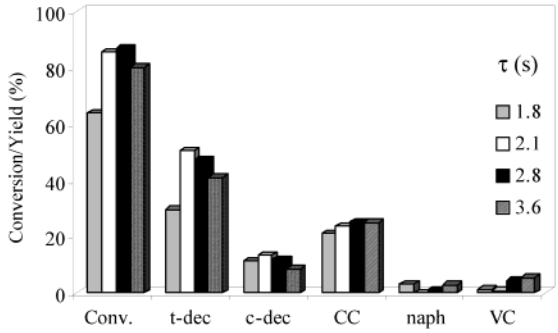

Figure 7. Conversion and yield as a function of the contact time on the Ni(Cit/A) catalyst. Experimental conditions: reaction temperature = 648 K, H_2/THN molar ratio = 10.1; $P(H_2)$ = 6 MPa.

hydrogenation products (*trans*- and *cis*-decalins) is higher at low reaction temperatures (Figure 6). On the other hand, the product distribution depends on the nickel salt used in the catalyst preparation. At high reaction temperatures, the formation of *cis*- and *trans*-decalin decays, and a concomitant increase in the formation of CCs was found. Thus, at 648 K, the yield of hydrogenation products for the Ni(Nit/E) and Ni(Nit/A) catalysts diminishes until 15% is reached, whereas for Ni(Cit/A) it is maintained at 50%. Moreover, the trans to cis yield ratio is higher for the Ni(Cit/A) catalyst, shifting from 7.3 to 5.0 when the reaction temperature varies between 548 and 648 K, whereas for Ni(Nit/E) and Ni(Nit/A), it changes from 2.6 to 2.2 and 3.4 to 2.3, respectively. The thermodynamics associated with the catalytic process favor the formation of *trans*-decalin,[25] which means that, at low temperatures, the *trans*- to *cis*-decalin ratio observed indicates that the hydrogenation process is governed by the thermodynamic equilibrium. However, the formation of CCs by the ring opening of tetralin and decalins is favored at high reaction temperatures. This is expected because the cracking reactions are endothermic and, hence, are favored at high temperatures.[54] This behavior is particularly important for the Ni(Cit/A) catalyst, which reaches a CC yield of 25% at 648 K. In all cases, the production of naphthalene was negligible. Interestingly, the yield of VC was only appreciable for the Ni(Nit/A) catalyst, which presented the highest acidity in its reduced form, but with a percentage as low as 2% at 648 K.

Therefore, the best catalytic performance is shown by the catalyst prepared by using nickel citrate, Ni(Cit/A). This behavior could be attributed to its suitable metallic properties in comparison with those of the catalysts obtained by using nickel nitrate solutions. This catalyst has demonstrated to be very active in the catalytic reaction studied with high yields of CC and hydrogenation products, 25 and 52%, respectively, at 648 K, together with a very low yield of VC. Moreover, the stability of this catalyst with the time on-stream is good, maintaining the conversion and selectivities for at least 6 h of reaction.

This catalytic study was completed by evaluating the influence of the contact time and the H_2/tetralin molar ratio on the conversion and selectivity toward hydrogenation and CC products. This was carried out by using the Ni(Cit/A) catalyst, which previously showed the best catalytic performance.

The effect of the contact time on the conversion and selectivity is shown in Figure 7. When this parameter

(52) Girgis, M. J.; Gates, B. C. *Ind. Eng. Chem. Res.* **1991**, *30*, 2021.
(53) Stanislaus, A.; Cooper, B. H. *Catal. Rev. Sci. Eng.* **1994**, *36*, 75.
(54) Yasuda, Y.; Yoshimura, Y. *Catal. Lett.* **1997**, *46*, 43.

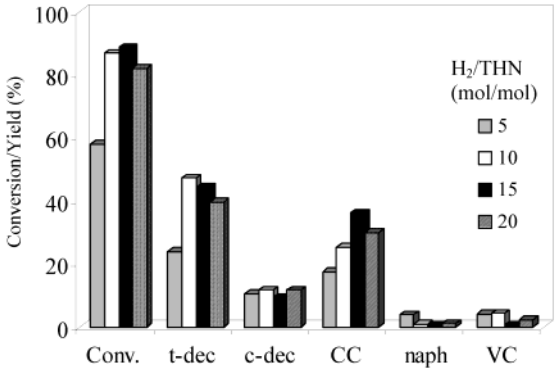

Figure 8. Conversion and yield as a function of the H_2/THN molar ratio on the Ni(Cit/A) catalyst. Experimental conditions: reaction temperature = 648 K; $P(H_2)$ = 6 MPa; contact time = 2.8 s.

was varied from 1.8 to 2.8 s, the conversion increases, but at 3.6 s of contact time, the conversion decreases again. At the lowest contact time (1.8 s), the low conversion is mainly due to the very limited production of *trans*-decalin. A contact time of 2.8 s was chosen for the study concerning the optimization of the H_2/tetralin molar ratio. This parameter is important because a high concentration of H_2 is necessary to overcome the thermodynamic limitations of the catalytic process,[16] but this implies elevated costs to recycle the excess H_2. It can be seen in Figure 8 that the conversion is drastically enhanced with the H_2/THN molar ratio, reaching the maximum value for a molar ratio of 15.0, and concomitantly, the highest yield of CCs (36.1%) is also achieved.

Conclusions

The use of nickel citrate, instead of nickel nitrate, as the nickel source for the preparation of nickel supported on zirconium-doped mesoporous silica, with a high nickel loading (ca. 20 wt %), allows highly active hydrogenation catalysts to be obtained. This catalyst shows a tetralin conversion close to 90% at 648 K and high yields of hydrogenation (*trans*- and *cis*-decalins) and CCs (53.8 and 36.1%, respectively). These values are obtained by using a H_2/tetralin molar ratio of 15 and a contact time of 2.8 s. This catalytic performance can be attributed to the suitable metallic properties of the active phase when nickel citrate is employed, with a very high metallic surface area due to the existence of very small metallic nickel particles on the surface of the mesoporous solid used as the support.

Acknowledgment. The financial support for this research was obtained under the project MAT2000-1144 (CICYT, Spain), for which we are very grateful. D.E.Q. also thanks the Ministerio de Ciencia y Tecnología for a fellowship.

LA020865L